# ON DERIVING OF SOME SIMPLE PLATE ELEMENTS

Jukka Aalto

Journal of Structural Mechanics
Vol. 40, No 4, 2007, pp. 55-79

## ABSTRACT

The paper presents a systematic and physically reasoned way of deriving the equations of some simple triangular and quadrilateral plate elements. The derivation is performed for Mindlin elements and the corresponding Kirchhoff elements are obtained as a special case. The starting point of the derivation is cubic approximation of the deflection and constant approximation of the tangential shear on the element sides. The connection of the derived elements with some existing ones is discussed. A numerical example to demonstrate the behavior of different versions of the elements is given.

## MOTIVATION WITH BEAM ELEMENTS

As an introduction to plate elements some aspects of beam elements are discussed shortly in the following. $C^1-$continuous, cubic finite element approximation

$$\tilde{v} = H_1 v_1 + H_2 v_{,x1} + H_3 v_2 + H_4 v_{,x2}\,, \tag{1}$$

is typically used to for the deflection $v(x)$ of an engineering beam element. Here $v_i$ and $v_{,xi}$ $(i=1,2)$ are the nodal deflections and the nodal derivatives of the deflection and $H_i$ $(i=1,\cdots,4)$ are cubic Hermitean shape functions. Because in a Bernoulli-Euler beam $v_{,x}=\theta$, where $\theta$ is the rotation of the beam, we can write $v_{,xi}=\theta_i$ $(i=1,2)$ and the deflection approximation can be expressed as

$$\tilde{v} = H_1 v_1 + H_2 \theta_1 + H_3 v_2 + H_4 \theta_2\,. \tag{2}$$

It is well known, that this element is nodally exact. This means that using it static finite element analysis of a uniform Bernoulli-Euler beam under any loading can produce exact nodal deflections and rotations.

The deflection approximation (1) can also be used to formulate a Timoshenko beam element as follows. In a Timoshenko beam $v_{,x} = \theta + \gamma$, where $\theta$ is the rotation and $\gamma$ is the shear[1]. Assuming the latter as constant within the element, we can write $v_{,xi} = \theta_i + \gamma$ ($i = 1, 2$). Consequently the deflection approximation of this Timoshenko beam element can be expressed as

$$\tilde{v} = H_1 v_1 + H_2 \theta_1 + H_3 v_2 + H_4 \theta_2 + (H_2 + H_4)\gamma \,. \tag{3}$$

An additional unknown, the shear $\gamma$ of the beam, is needed in this beam element. Because this parameter is separate within each element, it can be eliminated at the element level using static condensation. Thus final nodal parameters $w_i, \theta_i$ ($i = 1, 2$) of this element are the same as in the Bernoulli-Euler element. Also this element can be shown to be nodally exact.

An alternative elegant way of formulating a Timoshenko beam element is to use separate $C^0$ – continuous linear approximations

$$\tilde{v} = N_1 v_1 + N_2 v_2, \;\; \tilde{\theta} = N_1 \theta_1 + N_2 \theta_2 \,, \tag{4}$$

where $N_i$ are linear shape functions, for both the deflection $v(x)$ and the rotation $\theta(x)$. This Timoshenko beam element is not nodally exact but only approximate.

The 'nodally approximate' representation (4) is easily generalized to a plate and an approximation for the deflection and rotations inside the element can be obtained. Generalization of the 'nodally exact' representation (3) to a plate is more difficult. Here this difficulty is avoided by not trying to present the deflection inside the element but making assumptions to the deflection and the rotations on the element boundaries. For computing the internal virtual work it suffices, that we have approximations for the curvatures $\boldsymbol{\kappa}$ and the shears $\boldsymbol{\gamma}$ inside the element. For computing the loading terms a suitable approximation for the virtual deflection is still needed. In the numerical example of this paper linear and bilinear expressions are used for triangular and quadrilateral elements, respectively.

[1] The terms 'rotation' and 'shear' are used to denote the longer terms 'rotation of the normal' and 'transverse shear strain' in the following.

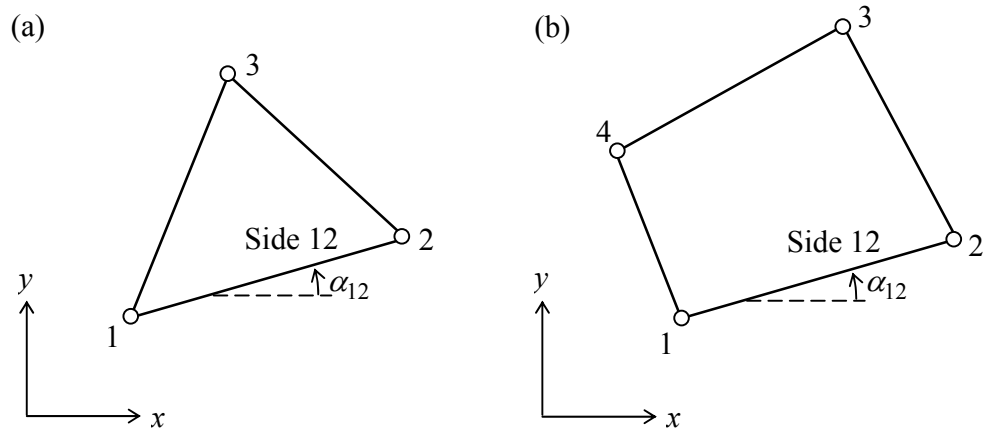


**Fig. 1:** (a) A three node triangular and (b) a four node quadrilateral element.

**SOME NOTATION**

We consider in this paper triangular and quadrilateral elements (Fig. 1) with three and four corner nodes, respectively. In the following we use the symbol $n$ ($n = 3$ or $n = 4$) for the number of corner nodes of the element. In order to perform the derivations in compact form, we consider a typical element side $ij$ or a typical node $j$, which is connected to element sides $ij$ and $jk$. After an equation corresponding to a typical element side $ij$ or a typical node $j$ has been obtained, it can be applied for all the element sides or nodes using cyclic permutation 1,2,3 or 1,2,3,4 of the indices $i, j,$ etc..

The length of a typical element side *ij* is

$$h_{ij} = \sqrt{(x_j - x_i)^2 + (y_j - y_i)^2} \,. \tag{5}$$

The cosine and sine of the direction angles of the element side $ij$ are

$$c_{ij} = \cos\alpha_{ij} = \frac{x_j - x_i}{h_{ij}},\ s_{ij} = \sin\alpha_{ij} = \frac{y_j - y_i}{h_{ij}}. \tag{6}$$

The nodal degrees of freedom of these elements are the nodal deflections $w_j$ and rotations $\theta_{xj}$ and $\theta_{yj}$ $j = 1,\cdots,n$. The tangential shears of the element sides $\gamma_s^{ij}$ have also special role in the following. The positive directions of these quantities are shown in Fig. 2.

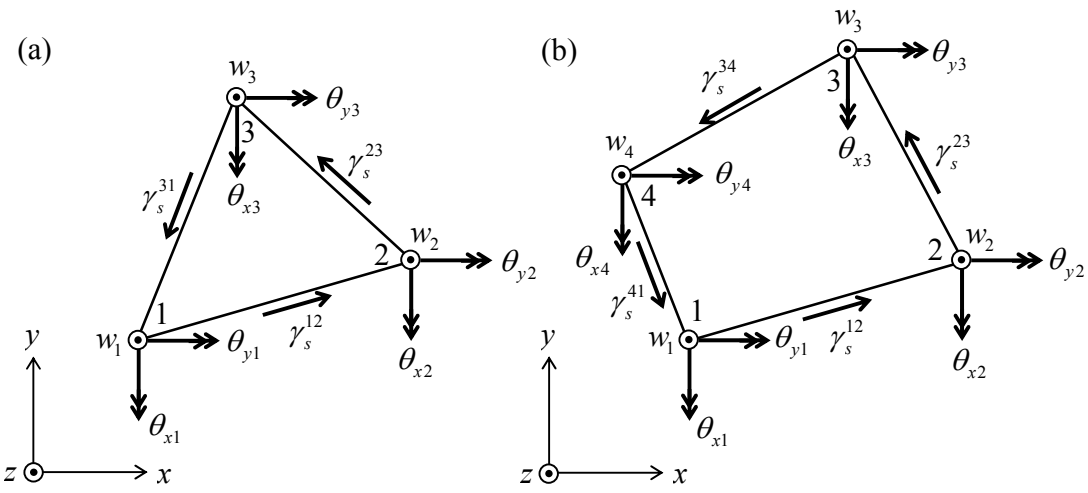


**Fig. 2:** Nodal deflections and rotations and tangential shears of element sides (a) triangle (b) quadrilateral

## ELEMENT KINEMATICS

### Assumptions

The starting point of the derivation of the plate elements of this paper is to (i) approximate the deflection and shear along the element sides as a cubic polynomial and a constant, respectively. Because such approximation is ideal in connection with both Bernoulli-Euler and Timoshenko beams, it is natural to use it along the sides of a plate element. Such plate elements suit well to practical structural analysis, because they can be easily and consistently combined with cubic beam elements.

In addition to the former there are three additional basic assumptions: (ii) the degrees of freedom of the element are the nodal deflections and rotations of the corner nodes and additional parameters for expressing the shear approximation, (iii) the normal component of the rotation is assumed to be distributed linearly along the element sides and (iv) the curvatures are assumed to be linear and bilinear within the triangular and quadrilateral element, respectively. The derivation of plate elements, which follows, has recently been proposed by *E.-M. Salonen* in a slightly different context [1].

### The curvatures at the nodes in terms of the nodal degrees of freedom and the shear parameters

The deflection $\tilde{w}(s)$ along the element side $ij$ is assumed to be cubic and of form (see (3))

$$\tilde{w}^{ij} = H_1 w_i + H_2(\theta_s^{ij})_i + H_3 w_j + H_4(\theta_s^{ij})_j + (H_2 + H_4)\gamma_s^{ij}, \tag{7}$$

where $w_i$ and $w_j$ are the deflections at nodes $i$ and $j$, respectively, $(\theta_s^{ij})_i$ and $(\theta_s^{ij})_j$ are the tangential components of the rotation of side $ij$ at nodes $i$ and $j$, respectively, and parameter $\gamma_s^{ij}$ is the tangential component of shear of side $ij$. With the help of the expression $\theta_s = w_{,s} - \gamma_s$ the tangential component of the rotation along an element side can also be expressed in terms of the same parameters and it can further be differentiated to get its tangential derivative $\theta_{s,s}$. Thus it is possible to get such tangential derivatives on sides $ij$ and $jk$ and further their values $(\theta_{s,s}^{ij})_j$ and $(\theta_{s,s}^{jk})_j$ at node $j$. Using the linearity assumption of the normal component of the rotation $\theta_n$ along element sides, it is possible to express its derivatives $(\theta_{n,s}^{ij})_j$ and $(\theta_{n,s}^{jk})_j$ at node $j$ in terms of the nodal rotations. Thereafter it is possible to express the Cartesian derivatives $(\theta_{x,x})_j$, $(\theta_{x,y})_j$, $(\theta_{y,x})_j$ and $(\theta_{y,y})_j$ of the rotation components at node $j$ in terms of the obtained derivatives $(\theta_{s,s}^{ij})_j$, $(\theta_{s,s}^{jk})_j$, $(\theta_{n,s}^{ij})_j$ and $(\theta_{n,s}^{jk})_j$. Finally the curvatures[2] at node $j$ can be evaluated using the expressions $\kappa_x = -\theta_{x,x}$, $\kappa_y = -\theta_{y,y}$ and $2\kappa_{xy} = -\theta_{x,y} - \theta_{y,x}$. With the help of the described sequence of operations the nodal curvatures $\kappa_{xj}$, $\kappa_{yj}$ and $2\kappa_{xyj}$ can be expressed as linear expressions of the nodal deflections, nodal rotations and the tangential shears of the element sides. Detailed derivation of the results is presented in appendix A. The resulting expression can be written as

$$\mathbf{k}^e = \mathbf{A}^e\mathbf{a}^e + \mathbf{B}^e\mathbf{b}^e, \tag{8}$$

where

$$\underset{3n\times 1}{\mathbf{k}^e} = \begin{Bmatrix} \kappa_{x1} \\ \kappa_{y1} \\ 2\kappa_{xy1} \\ \vdots \\ \kappa_{xn} \\ \kappa_{yn} \\ 2\kappa_{xyn} \end{Bmatrix}, \quad \underset{3n\times 1}{\mathbf{a}^e} = \begin{Bmatrix} w_1 \\ \theta_{y1} \\ \theta_{y1} \\ \vdots \\ w_n \\ \theta_{xn} \\ \theta_{yn} \end{Bmatrix} \tag{9}$$

[2] The term ‘curvatures’ is used to denote the longer term ‘curvatures and twist’ in the following

are the column vectors of the nodal curvatures, and nodal deflections and rotations, respectively. There are two possibilities of choosing the parameters $\mathbf{b}^e$ for expressing the shear approximation within the element. In the first version the parameters are the (constant) tangential shears of the element sides $\gamma_s^{ij}$. The number of these parameters is $n$ ($n=3$ triangle, $n=4$ quadrilateral). This case is called here $n-$parameter shear approximation. In the second more constrained case the shears are assumed to be constants $\gamma_x^e$ and $\gamma_y^e$, within the element. This case is called here $2-$parameter shear approximation. The parameters for the shear approximation are

$$\underset{n\times 1}{\mathbf{b}^e}=\begin{Bmatrix}\gamma_s^{12}\\ \vdots \\ \gamma_s^{n1}\end{Bmatrix},\ \underset{2\times 1}{\mathbf{b}^e}=\begin{Bmatrix}\gamma_x^e\\ \gamma_y^e\end{Bmatrix} \tag{10}$$

for the $n-$ and $2-$parameter shear approximations, respectively. The elements of matrices $\mathbf{A}^e$ and $\mathbf{B}^e$ are given in appendix A.

**The shears at the nodes in terms of the shear parameters**

It is possible to express nodal shears $\gamma_{xj}$ and $\gamma_{yj}$ at node $j$ as linear expressions of the tangential shears $\gamma_s^{ij}$ and $\gamma_s^{jk}$ of the element sides $ij$ and $jk$ (see Appendix B). This is the desired result for the $n-$parameter shear approximation. In the $2-$parameter shear approximation the nodal shears are simply $\gamma_{xj}=\gamma_x^e$ and $\gamma_{yj}=\gamma_y^e$. These results both for the $n-$ and $2-$parameter shear approximations can be written as

$$\mathbf{g}^e=\mathbf{C}^e\mathbf{b}^e, \tag{11}$$

where

$$\underset{2n\times 1}{\mathbf{g}^e}=\begin{Bmatrix}\gamma_{x1}\\ \gamma_{y1}\\ \vdots \\ \gamma_{xn}\\ \gamma_{yn}\end{Bmatrix} \tag{12}$$

the corresponding matrices $\mathbf{C}^e$ are given in appendix B.

**Approximation of the curvatures**

The distribution of the curvatures within the element is now assumed to be linear for a triangular element and bilinear for a quadrilateral element. Thus we can write

$$\tilde{\boldsymbol{\kappa}}(x,y) = \mathbf{N}_{\kappa}(x,y)\mathbf{k}^{e}, \tag{13}$$

where

$$\tilde{\boldsymbol{\kappa}} = \begin{Bmatrix} \tilde{\kappa}_x \\ \tilde{\kappa}_y \\ 2\tilde{\kappa}_{xy} \end{Bmatrix}, \tag{14}$$

$$\mathbf{N}_{\kappa} = \left[\mathbf{N}_{\kappa 1}, \cdots \mathbf{N}_{\kappa n}\right] \; n = 3 \text{ or } n = 4, \tag{15}$$

$$\mathbf{N}_{\kappa i} = N_i \mathbf{I}_{\kappa}, \tag{16}$$

$\mathbf{I}_{\kappa}$ is a $3\times 3$ unit matrix and $N_i$, $i = 1, \cdots, n$ are the corresponding linear or bilinear shape functions. Using equations (13) and (8), the curvatures approximation $\tilde{\boldsymbol{\kappa}}(x,y)$ can finally be expressed in terms of the nodal parameters $\mathbf{a}^{e}$ and the shear parameters $\mathbf{b}^{e}$ by

$$\tilde{\boldsymbol{\kappa}}(x,y) = \mathbf{N}_{\kappa}(x,y)\mathbf{A}^{e}\mathbf{a}^{e} + \mathbf{N}_{\kappa}(x,y)\mathbf{B}^{e}\mathbf{b}^{e}. \tag{17}$$

**Approximation of the shears**

The distribution of the shears within the element is also assumed to be linear for a triangular element and bilinear for a quadrilateral element. Thus we can write

$$\tilde{\boldsymbol{\gamma}}(x,y) = \mathbf{N}_{\gamma}(x,y)\mathbf{g}^{e}, \tag{18}$$

where

$$\tilde{\boldsymbol{\gamma}} = \begin{Bmatrix} \tilde{\gamma}_x \\ \tilde{\gamma}_y \end{Bmatrix}. \tag{19}$$

$$\mathbf{N}_{\gamma} = \left[\mathbf{N}_{\gamma 1}, \cdots \mathbf{N}_{\gamma n}\right] \; n = 3 \text{ or } n = 4, \tag{20}$$

$$\mathbf{N}_{\gamma i} = N_i \mathbf{I}_\gamma , \tag{21}$$

$\mathbf{I}_\gamma$ is a $2\times 2$ unit matrix and $N_i,\ i=1,\cdots,n$ are the corresponding linear or bilinear shape functions. Using equations (18) and (11), the shear approximation $\tilde{\boldsymbol{\gamma}}(x,y)$ can finally be expressed in terms of the element nodal parameters by

$$\tilde{\boldsymbol{\gamma}}(x,y) = \mathbf{N}_\gamma (x,y)\mathbf{C}^e \mathbf{b}^e . \tag{22}$$

## ELEMENT EQUATIONS OF THE PLATE ELEMENT

### General case

Internal virtual work of an elastic plate element is

$$\delta W^e_{\text{int}} = -\int_{A^e} (\delta\boldsymbol{\kappa}^T \mathbf{D}_\kappa \boldsymbol{\kappa} + \delta\boldsymbol{\gamma}^T \mathbf{D}_\gamma \boldsymbol{\gamma}) dA , \tag{23}$$

where

$$\mathbf{D}_\kappa = \begin{bmatrix} D^\kappa_{11} & D^\kappa_{12} & D^\kappa_{13} \\ D^\kappa_{21} & D^\kappa_{22} & D^\kappa_{23} \\ D^\kappa_{31} & D^\kappa_{32} & D^\kappa_{33} \end{bmatrix},\ \mathbf{D}_\gamma = \begin{bmatrix} D^\gamma_{11} & D^\gamma_{12} \\ D^\gamma_{21} & D^\gamma_{22} \end{bmatrix} \tag{24}$$

are the moment curvature matrix and the shear force shear matrix, which in the isotropic case are

$$\mathbf{D}_\kappa = \frac{Et^3}{12(1-\nu^2)} \begin{bmatrix} 1 & \nu & 0 \\ \nu & 1 & 0 \\ 0 & 0 & (1-\nu)/2 \end{bmatrix},\ \mathbf{D}_\gamma = kGt \begin{bmatrix} 1 & 0 \\ 0 & 1 \end{bmatrix}, \tag{25}$$

where $E$, $\nu$, $t$ and $G$ are modulus of elasticity, Poisson's ratio, thickness and shear modulus of the plate, respectively. Using the approximations (17) and (22) for both the virtual and actual curvatures and shears we get

$$\delta\tilde{W}_{\text{int}} = -\delta\mathbf{a}^{eT}(\mathbf{K}^e_{aa}\mathbf{a}^e + \mathbf{K}^{eT}_{ab}\mathbf{b}^e) - \delta\mathbf{b}^{eT}(\mathbf{K}^e_{ab}\mathbf{a}^e + \mathbf{K}^e_{bb}\mathbf{b}^e) \tag{26}$$

where

$$\begin{aligned}
\mathbf{K}^e_{aa} &= \mathbf{A}^{eT}\mathbf{k}^e_\kappa\mathbf{A}^e,\\
\mathbf{K}^e_{ab} &= \mathbf{B}^{eT}\mathbf{k}^e_\kappa\mathbf{A}^e,\\
\mathbf{K}^e_{bb} &= \mathbf{B}^{eT}\mathbf{k}^e_\kappa\mathbf{B}^e + \mathbf{C}^{eT}\mathbf{k}^e_\gamma\mathbf{C}^e,
\end{aligned} \tag{27}$$

and

$$\mathbf{k}^e_\kappa = \int_{A^e}\mathbf{N}^T_\kappa\mathbf{D}_\kappa\mathbf{N}_\kappa dA\,,\quad \mathbf{k}^e_\gamma = \int_{A^e}\mathbf{N}^T_\gamma\mathbf{D}_\gamma\mathbf{N}_\gamma dA\,. \tag{28}$$

If $\mathbf{D}_\kappa$ and $\mathbf{D}_\gamma$ are assumed to be constants within the element, these matrices can further be written as

$$\underset{3n\times 3n}{\mathbf{k}^e_\kappa} = \begin{bmatrix} m_{11}\mathbf{D}_\kappa & \cdots & m_{1n}\mathbf{D}_\kappa \\ \vdots & \ddots & \vdots \\ m_{n1}\mathbf{D}_\kappa & \cdots & m_{nn}\mathbf{D}_\kappa \end{bmatrix},\quad \underset{3n\times 3n}{\mathbf{k}^e_\gamma} = \begin{bmatrix} m_{11}\mathbf{D}_\gamma & \cdots & m_{1n}\mathbf{D}_\gamma \\ \vdots & \ddots & \vdots \\ m_{n1}\mathbf{D}_\gamma & \cdots & m_{nn}\mathbf{D}_\gamma \end{bmatrix} \tag{29}$$

where the coefficients $m_{ij}$ are

$$m_{ij} = \int_{A^e} N_i N_j dA,\ i,j = 1,\cdots,n \tag{30}$$

and can be obtained using numerical integration. In connection with triangular and quadratic elements the 3 point rule and the $2\times 2$ Gauss quadratures are needed for integration, respectively. Because of symmetry ($m_{ij} = m_{ji}$) only 6 or 10 integrations per element need to be performed in connection with triangular ($n = 3$) and quadrilateral elements ($n = 4$), respectively. Also analytical expressions for the coefficients $m_{ij}$ for a triangular element can easily be written. Using equations (27) the matrices $\mathbf{K}^e_{aa}$, $\mathbf{K}^e_{ab}$ and $\mathbf{K}^e_{bb}$ can be computed quite efficiently.

**Static condensation**

If the shear parameters $\mathbf{b}^e$ are distinct within each element, it is possible to eliminate them using static condensation on the element level. The finite element equations corresponding to virtual parameters $\delta\mathbf{b}^e$ are

$$\mathbf{K}_{ab}^{e}\mathbf{a}^{e}+\mathbf{K}_{bb}^{e}\mathbf{b}^{e}=\mathbf{R}_{b}^{e}, \tag{31}$$

where $\mathbf{R}_{b}^{e}$ is the corresponding element load vector. Because now the shear parameters $\mathbf{b}^{e}$ belong only to the element under consideration, they can be solved resulting to

$$\mathbf{b}^{e}=-\mathbf{K}_{bb}^{e-1}\mathbf{K}_{ab}^{e}\mathbf{a}^{e}+\mathbf{K}_{bb}^{e-1}\mathbf{R}_{b}^{e}. \tag{32}$$

Substituting these and the corresponding virtual parameters $\delta\mathbf{b}^{e}=-\mathbf{K}_{bb}^{e-1}\mathbf{K}_{ab}^{e}\delta\mathbf{a}^{e}$ into the expression (26) of the internal virtual work of the element gives

$$\delta\tilde{W}_{\text{int}}=-\delta\mathbf{a}^{eT}\mathbf{K}^{e}\mathbf{a}^{e}, \tag{33}$$

where

$$\mathbf{K}^{e}=\mathbf{K}_{aa}^{e}-\mathbf{K}_{ab}^{eT}\mathbf{K}_{bb}^{e-1}\mathbf{K}_{ab}^{e}. \tag{34}$$

This is now the element stiffness matrix of the condensed problem and the element degrees of freedom are the nodal parameters $\mathbf{a}^{e}$.

## EXAMPLE PROBLEM

In order to demonstrate the behavior of the different element types, which can be developed as special cases of the present formulation, a clamped circular plate of Fig. 3 under uniform load is used as a simple example problem in the following.

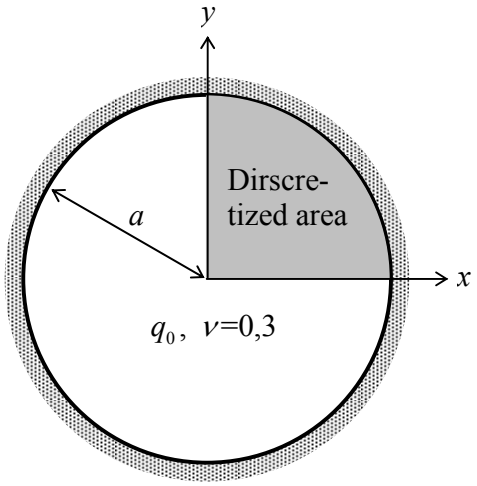


**Fig. 3:** Clamped circular plate of radius *a* under uniform load $q_0$

Both Kirchhoff and Mindlin plates are considered. In the Kirchhoff case the bending stiffness of the plate is $D$ and in the Mindlin case the bending and shear stiffnesses are $D_\kappa$ and $D_\gamma$, respectively. A dimensionless ratio $\varepsilon = D_\kappa /(D_\gamma a^2)$ is used to control the relative sizes of the bending and shear stiffness.

Because analytical solution of this problem both in the Kirchhoff and Mindlin cases is available, relative energy norm $\eta_{\mathrm{E}}$ of the error of the finite element analysis [2] can be computed. Experimental convergence plots of the relative error in energy $\eta_{\mathrm{E}}$ [%] in terms of the relative mesh size $h/a$ are used in the following to compare the behavior of the different formulations under consideration. Typical grids of triangular and quadrilateral elements used in the convergence study are shown in Fig. 4.

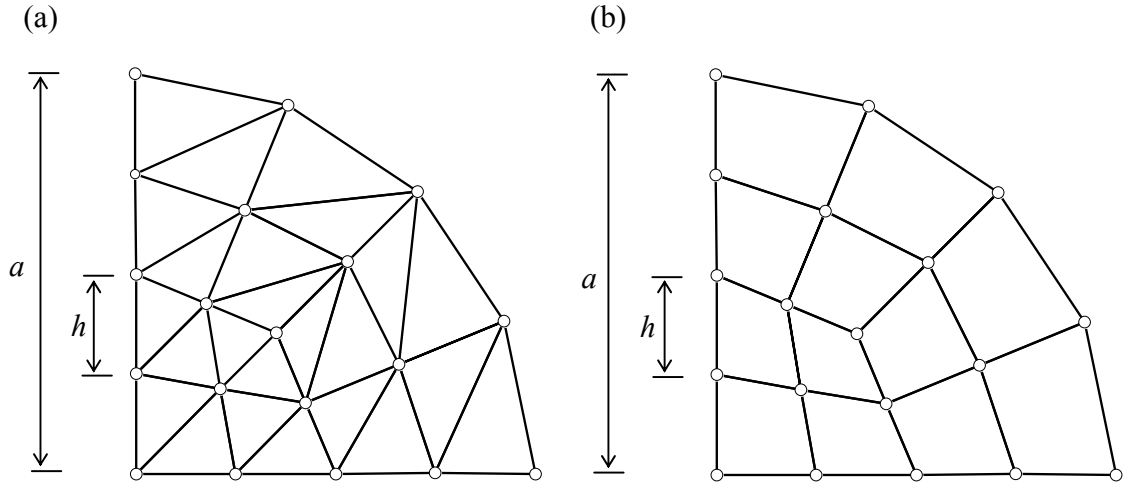


**Fig. 4:** Typical grids ( $h/a = 1/4$ ) of (a) triangular and (b) quadrilateral elements

## DIFFERENT ELEMENT TYPES AS SPECIAL CASES OF THE FORMULATION

### Kirchhoff plate elements

Kirchhoff plate elements of the presented formulation can be easily obtained by assuming the shears to vanish. Substituting $\mathbf{b}^e = \mathbf{0}$ into the expression (26) of the internal virtual work of the element gives

$$\delta \tilde{W}_{\mathrm{int}} = -\delta \mathbf{a}^{eT} \mathbf{K}^e_{aa} \mathbf{a}^e . \tag{35}$$

Thus the stiffness matrix of the element is simply

$$\mathbf{K}^e = \mathbf{K}^e_{aa} . \tag{36}$$

The element degrees of freedom of the element are the nodal parameters $\mathbf{a}^e$, i.e. the nodal deflections and rotations of the corner nodes.

The developed triangular element proves out to be the well-known discrete Kirchhoff triangular (DKT) element (see for example reference [3]). This is be seen as follows: In the DKT-element (i) the deflection is assumed to be cubic along the element sides, (ii) the degrees of freedom are the nodal deflections and rotations of the corner nodes, (iii) the normal rotations are assumed to be linear along the element sides and (iv) the approximation of the rotations, which is consistent with the nodal parameters, is quadratic. The first three assumptions hold also for this element. The approximation of the curvatures of the DKT-element is obtained simply by differentiating the rotations. Because the geometry of the triangular element is linear, this differentiation results to linear expressions of the curvatures. This assumption was also made in the presented formulation.

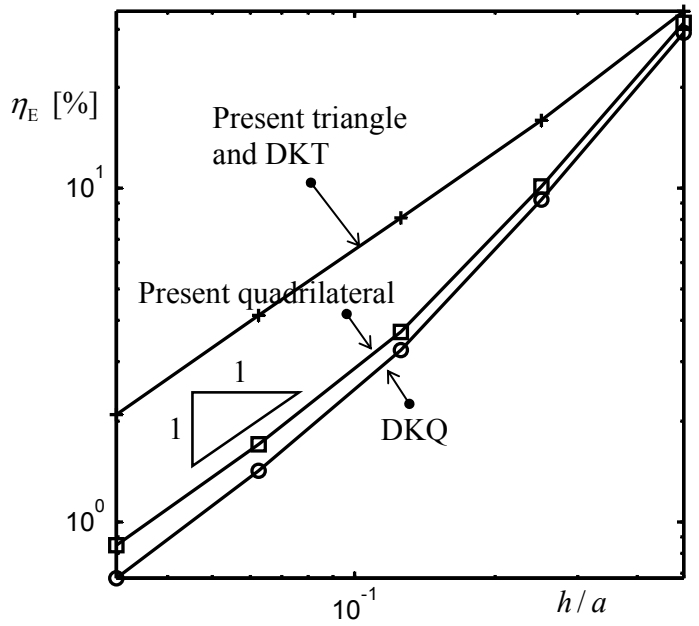


**Fig. 5:** Experimental convergence plot of the error in energy of the Kirchhoff plate elements

Comparison of the present quadrilateral element with the discrete Kirchhoff quadrilateral (DKQ) element [4] proceeds as follows: The first three assumptions hold for both elements. The fourth assumption of the DKQ-element states that the rotations are biquadratic. Because the geometry of the quadrilateral element is bilinear (not linear), differentiation of

the biquadratic rotations does not result to bilinear curvatures. Thus the present element is not equivalent to the DKQ-element.

The derived equations (27a) and (29a) and (30) for computing the element stiffness matrix (36) are automatically in an efficient form. Similar form of the stiffness matrix of a triangular DKT element has been proposed in reference [5].

Fig. 5 shows experimental convergence study of the present Kirchhoff triangular and quadrilateral elements. The corresponding results of the DKT and DKQ elements are also shown for comparison. The experimental rate of convergence, which is the slope of the curve, is approximately 1 for all the element types.

**Mindlin plate elements**

Continuous $n-$parameter shear approximation

In this case the tangential shears on the element boundaries are common and system degrees of freedom $\mathbf{b}$ of the problem. The system equations of the problem are

$$\begin{aligned} \mathbf{K}_{aa}\mathbf{a} + \mathbf{K}_{ab}^{T}\mathbf{b} &= \mathbf{R}_{a}, \\ \mathbf{K}_{ab}\mathbf{a} + \mathbf{K}_{bb}\mathbf{b} &= \mathbf{R}_{b}, \end{aligned} \tag{37}$$

where $\mathbf{K}_{aa}$, $\mathbf{K}_{ab}$, $\mathbf{K}_{bb}$ are the system matrices corresponding to the element matrices (27) and $\mathbf{R}_{a}$ and $\mathbf{R}_{b}$ are the system load vectors. The final unknowns of this formulation are both the nodal deflections and rotations $\mathbf{a}$ and the tangential shears of the element boundaries $\mathbf{b}$. It is important to specify unique positive directions to the system degrees of freedom $\mathbf{b}$. One choice is to keep the direction from lower to higher system node number as positive. This choice must be properly handled in the assembly process.

The main idea behind this Mindlin element was first proposed by *E.-M. Salonen* in References [6] and [7] in connection with a special triangular plate bending element. The same idea has further been applied in a technique, by which existing Kirchhoff plate elements can be extended to handle Mindlin plates [8].

Fig. 6 presents experimental convergence results obtained using the present quadrilateral Mindlin elements with continuous $4-$parameter shear approximation. The three values of the dimensionless stiffness ratio $\varepsilon$ cover the whole range of such values possible in practical applications. The values $\varepsilon = 10$ and $\varepsilon = 10^{-3}$ correspond to a sandwich plate and a very thin plate, respectively. Figs. 7 presents similar results obtained using the present triangular Mindlin elements with continuous $3-$parameter shear approximation. It is

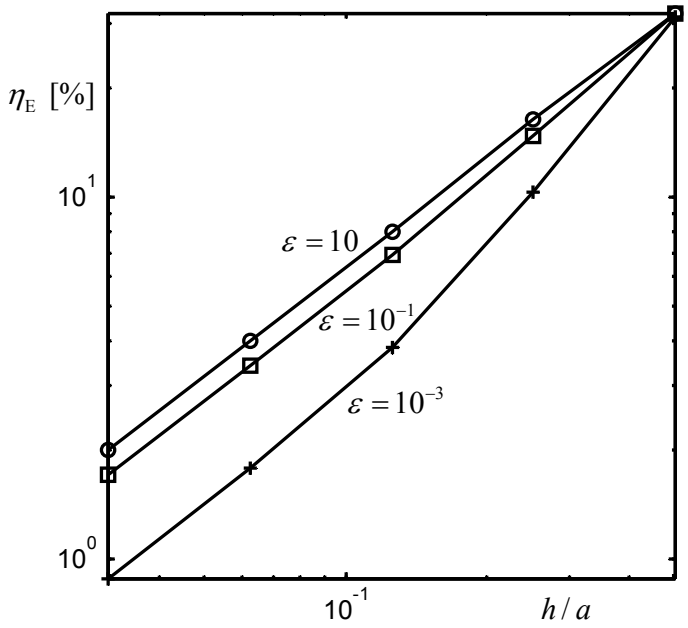


**Fig. 6:** Experimental convergence plot of the error in energy of the Mindlin plate elements: quadrilaterals, continuous 4 – parameter shear approximation

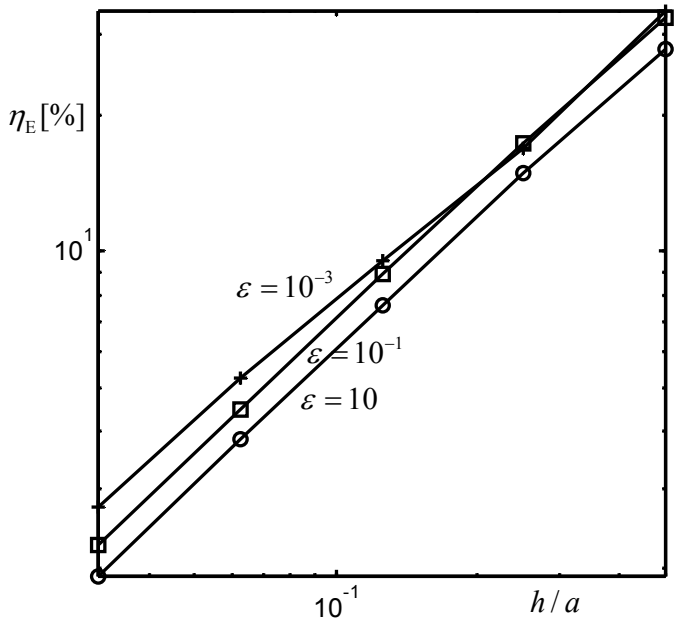


**Fig. 7:** Experimental convergence plot of the error in energy of the Mindlin plate elements: triangles, continuous 3 – parameter shear approximation

important to note that both elements behave well both in connection with shear flexible sandwich plates and in thin plates.

Discontinuous $n-$parameter ( $n = 3$ or $4$ ) shear approximation

In this case the tangential shears of neighboring elements are not constrained to be equal along opposite element sides. Thus the parameters $\mathbf{b}^e$, which describe the shear approximation, are distinct form element to element and can be eliminated by static condensation. The final unknowns are thus the nodal deflections and rotations $\mathbf{a}$. The draw-back of this formulation is loss of continuity of the deflection on the element boundaries. The deflection is, however, point-wise continuous in addition to the end nodes also at the centers of the element sides[3]. A technique of generalizing the DKT and DKQ plate elements to Mindlin plates by using such discontinuous $n-$parameter shear approximations has bee presented in Reference [9] and [10]. In these papers the equations, which are used to eliminate the shear parameters in the element level, have been formulated differently.

$2-$parameter shear approximation

Also in this case the tangential shears are discontinuous on the element boundaries, and the two shear parameters can be eliminated by static condensation. The final unknowns are thus the nodal deflections and rotations $\mathbf{a}$. Techniques of generalizing the DKT plate element to Mindlin plates by using such $2-$parameter shear approximation has bee proposed in Reference [11] and [12]. Also in these papers the local elimination of the shear parameters has been formulated differently.

Numerical comparison

Figs. 8 and 9 present comparison of the three variations of the shear approximation in connection with quadrilateral and triangular elements, respectively. The continuous $n-$parameter shear approximation works well. The discontinuous $n-$parameter shear approximation seems to give almost identical results in the simple example problem considered. In connection with quadrilateral elements, the two parameter model does not converge, but in connection with triangular elements, it gives acceptable results.

[3] The discontinuity is caused by the coefficient $N_2 + N_4$ of $\gamma_{ij}^e$ in equation (7). It is easy to see using equation (A2) of appendix A, that this coefficient is zero, when $\xi = 0,\ 1/2$ and $1$.

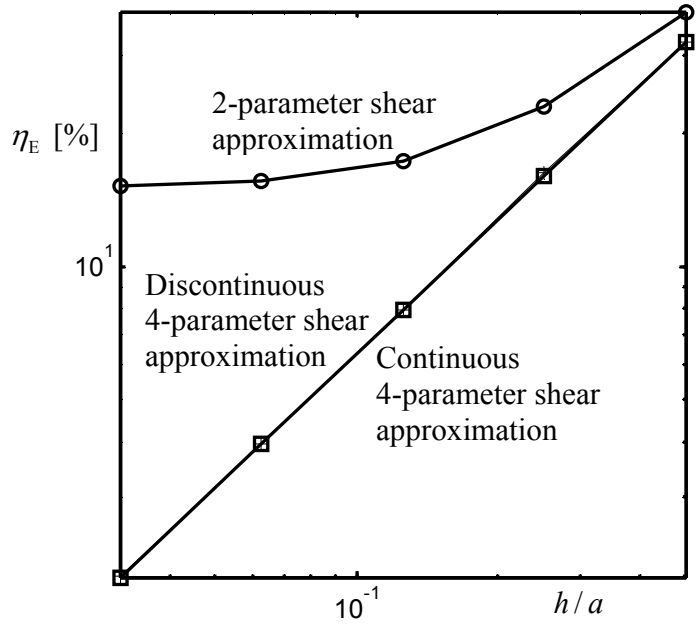


**Fig 8:** Experimental convergence plot of the error in energy of the Mindlin quadrilateral plate elements: Comparison of the three variations of the shear approximation

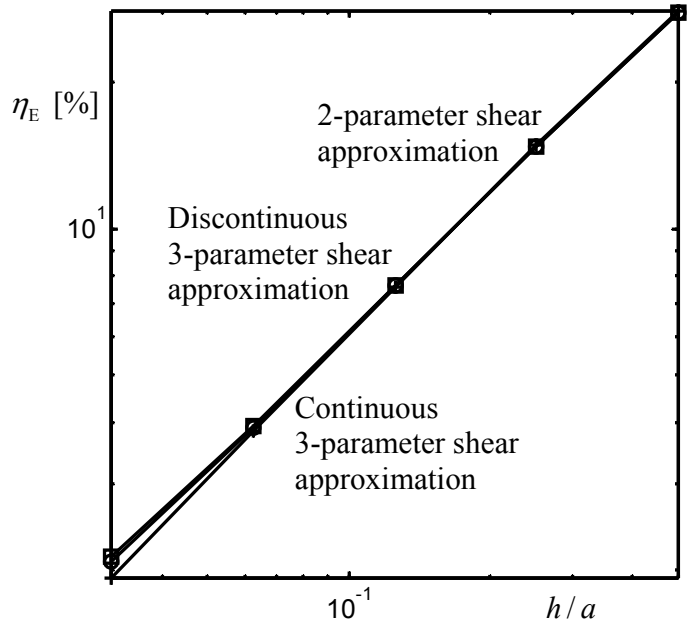


**Fig 9:** Experimental convergence plot of the error in energy of the Mindlin triangular plate elements: Comparison of the three variations of the shear approximation

## CONCLUSIONS

A physically reasoned way of deriving special triangular and quadrilateral plate elements was presented. The starting point of the derivation is cubic approximation of the deflection and constant approximation of the tangential shear along the element sides. The curvatures inside the elements are linear and bilinear for triangles and quadrilaterals, respectively. The degrees of freedom are the deflections and rotations at the corner nodes and additional shear parameters in the Mindlin case. In four of the six Mindlin elements presented, the shear parameters are eliminated at the element level.

All the presented element types were implemented in this work. In order to get an idea, how they behave, a clamped circular plate under uniform load was used as a simple numerical example. Experimental convergence studies of the error in energy were performed. Main results of these studies show, that the all but one (quadrilateral Mindlin element with 2-parameter shear approximation) of the element types seem to converge. The accuracy of the Kirchoff elements and the (converging) Mindlin elements is quite comparable. Because the Mindlin elements with distinct shear parameters are more effective and easier to implement than those with continuous shear, it can be concluded, that the Mindlin triangle with 2-parameter shear approximation and the Mindlin quadrilateral with discontinuous 4-parameter shear approximation seem to be most effective of the Mindlin elements studied in this paper.

## ACKNOWLEDGEMENT

Comments of suggestions of emeritus professor *Eero-Matti Salonen* in this work and many others are gratefully acknowledged. His long lasting co-operation, encouragement and friendship have been irreplaceable.

## REFERENCES

1. J. Aalto and E.-M. Salonen, Post-processing Reissner-Mindlin plate finite elements, Report 3, Helsinki University of Technology, Structural Mechanics. (Under preparation.)

2. O.C. Zienkiewicz and R. L. Taylor, The Finite Element Method, Fourth Edition, Vol.1 Basic Formulation and Linear Problems, McGraw-Hill, 1989, pp. 398-407.

3. J. L. Batoz, K. J. Bathe, and L. W. Ho, A study of three-node plate bending elements, Int. j. numer. methods eng., **15**, 1980, pp. 1771-1812.

4. J. L. Batoz, K and M. Ben Tahar, Evaluation of a new quadrilateral thin plate bending element, Int. j. numer. methods eng., **18**, 1982, pp. 1655-1677.

5. C. Jeyachandrabose, J. Kirkhope and C. Rames Baby, An alternative explicit formulation for the DKT plate-bending element, Int. j. numer. methods eng., **21** 1985, pp. 1289-1293.

6. J. Aalto and E.-M. Salonen, A triangular non-conforming plate bending element, Proceedings of the 2nd Finnish Mechanics Days, Report 29 (Ed. A. Pramila), Tampere, 1985, pp. 53-59.

7. J. Aalto and E.-M. Salonen, A triangular non-conforming plate bending element, Publication No. 22, Helsinki University of Technology, Mechanics, 1986, 71 p.

8. J. Aalto, From Kirchhoff to Mindlin plate elements, Communications in Applied Numerical Methods, Vol. 4, pp. 231-241, (1988)

9. I. Katili, A new discrete Kirchhoff-Mindlin element based on Mindlin-Reissner plate theory and assumed shear strain fields – part I: An extended DKT element for thick-plate bending analysis, Int. j. numer. methods eng., **36** 1993, pp. 1859-1883.

10. I. Katili, A new discrete Kirchhoff-Mindlin element based on Mindlin-Reissner plate theory and assumed shear strain fields – part II: An extended DKQ element for thick-plate bending analysis, Int. j. numer. methods eng., **36** 1993, pp. 1885-1908.

11. J. L. Batoz and P. Lardeur, A discrete shear triangular nine D.O.F. element for the analysis of thick to very thin plates, Int. j. numer. methods eng., **28** 1989, pp. 533-560.

12. J. L. Batoz and I. Katili, On a simple triangular Reissner/Mindlin plate element based on incompatible modes and discrete constraints. Int. j. numer. methods eng., **32** 1992, pp. 1603-1632.

**Appendix A:** The nodal curvatures in terms of the nodal deflections, nodal rotations and the parameters for expressing the shears

Consider first a vector $\mathbf{v}$, which can be the rotation vector $\boldsymbol{\theta}$, the shear vector $\boldsymbol{\gamma}$ or the gradient of a scalar function. The Cartesian components and the tangential and normal components of an element side of this vector are $v_x$, $v_y$ and $v_s$, $v_n$, respectively. The relations between these components in connection with a typical element side $ij$ (see Fig. 1) can be written as

$$\begin{cases} v_s^{ij} = c_{ij} v_x + s_{ij} v_y, \\ v_n^{ij} = s_{ij} v_x - c_{ij} v_y. \end{cases} \tag{A1}$$

We assume the deflection $w$ along the element side $ij$ to be cubic polynomial (7) and the shear component $\gamma_s^{ij}$ to be a constant. The cubic Hermitean shape functions in this expression are

$$\begin{aligned} &H_1 = 1 - 3\xi^2 + 2\xi^3,\ H_2 = (\xi - 2\xi^2 + \xi^3) h_{ij}, \\ &H_3 = 3\xi^2 - 2\xi^3,\ H_4 = (-\xi^2 + \xi^3) h_{ij} \end{aligned} \tag{A2}$$

where $\xi$ is a natural co-ordinate such that $\xi = 0$ and $\xi = 1$ at nodes *i* and *j*, respectively. Using the expression $\theta_s = w_{,s} - \gamma_s$ of the tangential rotation $\theta_s$ of the plate, where $w_{,s} \equiv dw/ds$, the approximation of the tangential rotation of side $ij$ gets the form

$$\tilde{\theta}_s^{ij} = H_1' w_i + H_2' (\theta_s^{ij})_i + H_3' w_j + H_4' (\theta_s^{ij})_j + (H_2' + H_4' - 1) \gamma_s^{ij}, \tag{A3}$$

where $H_k' = dH_k / ds$ $(k = 1, \cdots, 4)$. Differentiating this with respect to the tangential co-ordinate *s* gives

$$\tilde{\theta}_{s,s}^{ij} = H_1'' w_i + H_2'' (\theta_s^{ij})_i + H_3'' w_j + H_4'' (\theta_s^{ij})_j + (H_2'' + H_4'') \gamma_s^{ij}, \tag{A4}$$

where $H_k'' = d^2 H_k / ds^2$. The values of this derivative at the element nodes *i* and *j* can now be obtained and they are

$$
\begin{aligned}
(\theta^{ij}_{s,s})_i &\equiv \theta^{ij}_{s,s}(0) = -\frac{6}{h^2_{ij}} w_i - \frac{4}{h_{ij}} (\theta^{ij}_s)_i + \frac{6}{h^2_{ij}} w_j - \frac{2}{h_{ij}} (\theta^{ij}_s)_j - \frac{6}{h_{ij}} \gamma^{ij}_s , \\
(\theta^{ij}_{s,s})_j &\equiv \theta^{ij}_{s,s}(1) = +\frac{6}{h^2_{ij}} w_i + \frac{2}{h_{ij}} (\theta^{ij}_s)_i - \frac{6}{h^2_{ij}} w_j + \frac{4}{h_{ij}} (\theta^{ij}_s)_j + \frac{6}{h_{ij}} \gamma^{ij}_s .
\end{aligned}
\tag{A5}
$$

Expressing further the tangential rotations $(\theta^{ij}_s)_i$, $(\theta^{ij}_s)_j$ of the nodes $i$ and $j$ in terms of the nodal rotations $\theta_{xi}$, $\theta_{yi}$, $\theta_{xj}$, $\theta_{xj}$, using the first equation (A1), equations (A5) reduce to

$$
\begin{aligned}
(\theta^{ij}_{s,s})_i &= -\frac{6}{h^2_{ij}} w_i - \frac{4c_{ij}}{h_{ij}} \theta_{xi} - \frac{4s_{ij}}{h_{12}} \theta_{yi} + \frac{6}{h^2_{ij}} w_j - \frac{2c_{ij}}{h_{ij}} \theta_{xj} - \frac{2s_{ij}}{h_{ij}} \theta_{yj} - \frac{6}{h_{ij}} \gamma^{ij}_s , \\
(\theta^{ij}_{s,s})_j &= +\frac{6}{h^2_{1ij}} w_i + \frac{2c_{ij}}{h_{ij}} \theta_{xi} + \frac{2s_{ij}}{h_{12}} \theta_{yi} - \frac{6}{h^2_{ij}} w_j + \frac{4c_{ij}}{h_{ij}} \theta_{xj} + \frac{4s_{ij}}{h_{ij}} \theta_{yj} + \frac{6}{h_{ij}} \gamma^{ij}_s .
\end{aligned}
\tag{A6}
$$

These equations express the nodal derivatives of the tangential rotations in terms of the nodal deflections, rotations and tangential shears of the $n-$parameter shear approximation. In the $2-$parameter shear approximation we still have to express the shear of the element side $\gamma^{ij}_s$ in terms of the element shears $\gamma^e_x$ and $\gamma^e_y$, using the first equation (A1). The result is slightly different and of form

$$
\begin{aligned}
(\theta^{ij}_{s,s})_i &= -\frac{6}{h^2_{ij}} w_i - \frac{4c_{ij}}{h_{ij}} \theta_{xi} - \frac{4s_{ij}}{h_{12}} \theta_{yi} + \frac{6}{h^2_{ij}} w_j - \frac{2c_{ij}}{h_{ij}} \theta_{xj} - \frac{2s_{ij}}{h_{ij}} \theta_{yj} - \frac{6c_{ij}}{h_{ij}} \gamma^e_x - \frac{6s_{ij}}{h_{ij}} \gamma^e_y . \\
(\theta^{ij}_{s,s})_j &= +\frac{6}{h^2_{1ij}} w_i + \frac{2c_{ij}}{h_{ij}} \theta_{xi} + \frac{2s_{ij}}{h_{12}} \theta_{yi} - \frac{6}{h^2_{ij}} w_j + \frac{4c_{ij}}{h_{ij}} \theta_{xj} + \frac{4s_{ij}}{h_{ij}} \theta_{yj} + \frac{6c_{ij}}{h_{ij}} \gamma^e_x + \frac{6s_{ij}}{h_{ij}} \gamma^e_y .
\end{aligned}
\tag{A7}
$$

Consider next normal component of the rotation $\theta_n$ and assume, that it is distributed linearly along the element sides. Thus with the help of the second equation (A1) the derivatives of $\theta_n$ along side $ij$ at both ends $i$ and $j$ of the side get the form

$$
(\theta^{ij}_{n,s})_i = (\theta^{ij}_{n,s})_j = \frac{1}{h_{ij}} [-(\theta^{ij}_n)_i + (\theta^{ij}_n)_j] = -\frac{s_{ij}}{h_{ij}} \theta_{xi} + \frac{c_{ij}}{h_{ij}} \theta_{yi} + \frac{s_{ij}}{h_{ij}} \theta_{xj} - \frac{c_{ij}}{h_{ij}} \theta_{yj} . \tag{A8}
$$

Next we start to consider a typical side $ij$ of the element and with the help of first equation (A1) get for the tangential derivatives of the rotation components $\theta_s$ and $\theta_n$ on this side

$$\begin{aligned}
\frac{\partial \theta_s^{ij}}{\partial s} &= \frac{\partial}{\partial s}(c_{ij}\theta_x^{ij} + s_{ij}\theta_y^{ij}) = c_{ij}\frac{\partial}{\partial x}(c_{ij}\theta_x^{ij} + s_{ij}\theta_y^{ij}) + s_{ij}\frac{\partial}{\partial y}(c_{ij}\theta_x^{ij} + s_{ij}\theta_y^{ij}) \\
&= c_{ij}c_{ij}\theta_{x,x}^{ij} + s_{ij}c_{ij}\theta_{x,y}^{ij} + c_{ij}s_{ij}\theta_{y,x}^{ij} + s_{ij}s_{ij}\theta_{y,y}^{ij} \\
\frac{\partial \theta_n^{ij}}{\partial s} &= \frac{\partial}{\partial s}(s_{ij}\theta_{x,s}^{ij} - c_{ij}\theta_{y,s}^{ij}) = c_{ij}\frac{\partial}{\partial x}(s_{ij}\theta_x^{ij} - c_{ij}\theta_y^{ij}) + s_{ij}\frac{\partial}{\partial y}(s_{ij}\theta_x^{ij} - c_{ij}\theta_y^{ij}) \\
&= c_{ij}s_{ij}\theta_{x,x}^{ij} + s_{ij}s_{ij}\theta_{x,y}^{ij} - c_{ij}c_{ij}\theta_{y,x}^{ij} - s_{ij}c_{ij}\theta_{y,y}^{ij}
\end{aligned} \tag{A.9}$$

Writing these equations at node $j$ corresponding to both side $ij$ and side $jk$ we further get

$$\begin{aligned}
(\theta_{s,s}^{ij})_j &= c_{ij}c_{ij}(\theta_{x,x})_j + s_{ij}c_{ij}(\theta_{x,y})_j + c_{ij}s_{ij}(\theta_{y,x})_j + s_{ij}s_{ij}(\theta_{y,y})_j, \\
(\theta_{n,s}^{ij})_j &= c_{ij}s_{ij}(\theta_{x,x})_j + s_{ij}s_{ij}(\theta_{x,y})_j - c_{ij}c_{ij}(\theta_{y,x})_j - s_{ij}c_{ij}(\theta_{y,y})_j, \\
(\theta_{s,s}^{jk})_j &= c_{jk}c_{jk}(\theta_{x,x})_j + s_{jk}c_{jk}(\theta_{x,y})_j + c_{jk}s_{jk}(\theta_{y,x})_j + s_{jk}s_{jk}(\theta_{y,y})_j, \\
(\theta_{n,s}^{jk})_j &= c_{jk}s_{jk}(\theta_{x,x})_j + s_{jk}s_{jk}(\theta_{x,y})_j - c_{jk}c_{jk}(\theta_{y,x})_j - s_{jk}c_{jk}(\theta_{y,y})_j.
\end{aligned} \tag{A.10}$$

This linear set of equations can be solved for the nodal derivatives of the rotations $\theta_x$ and $\theta_y$ at node $j$ resulting to

$$\begin{aligned}
(\theta_{x,x})_j &= 1/d_j[+c_{ij}s_{jk}(\theta_{s,s}^{ij})_j + s_{ij}s_{jk}(\theta_{n,s}^{ij})_j - s_{ij}c_{jk}(\theta_{s,s}^{jk})_j - s_{ij}s_{jk}(\theta_{n,s}^{jk})_j], \\
(\theta_{x,y})_j &= 1/d_j[-c_{ij}c_{jk}(\theta_{s,s}^{ij})_j - s_{ij}c_{jk}(\theta_{n,s}^{ij})_j + c_{ij}c_{jk}(\theta_{s,s}^{jk})_j + c_{ij}s_{jk}(\theta_{n,s}^{jk})_j], \\
(\theta_{y,x})_j &= 1/d_j[+s_{ij}s_{jk}(\theta_{s,s}^{ij})_j - c_{ij}s_{jk}(\theta_{n,s}^{ij})_j - s_{ij}s_{jk}(\theta_{s,s}^{jk})_j + s_{ij}c_{jk}(\theta_{n,s}^{jk})_j], \\
(\theta_{y,y})_j &= 1/d_j[-s_{ij}c_{jk}(\theta_{s,s}^{ij})_j + c_{ij}c_{jk}(\theta_{n,s}^{ij})_j + c_{ij}s_{jk}(\theta_{s,s}^{jk})_j - c_{ij}c_{jk}(\theta_{n,s}^{jk})_j],
\end{aligned} \tag{A11}$$

where

$$d_j = c_{ij}s_{jk} - s_{ij}c_{jk}. \tag{A12}$$

Substituting these into the expressions

$$\kappa_{xj} = -(\theta_{x,x})_j,\ \kappa_{yj} = -(\theta_{y,y})_j,\ 2\kappa_{xyj} = -(\theta_{x,y})_j - (\theta_{y,x})_j \tag{A13}$$

of the nodal curvatures at node $j$ we first get

$$\kappa_{xj} = \frac{1}{d_j}[-c_{ij}s_{jk}(\theta^{ij}_{s,s})_j - s_{ij}s_{jk}(\theta^{ij}_{n,s})_j + s_{ij}c_{jk}(\theta^{jk}_{s,s})_j + s_{ij}s_{jk}(\theta^{jk}_{n,s})_j],$$

$$\kappa_{yj} = \frac{1}{d_j}[+s_{ij}c_{jk}(\theta^{ij}_{s,s})_j - c_{ij}c_{jk}(\theta^{ij}_{n,s})_j - c_{ij}s_{jk}(\theta^{jk}_{s,s})_j + c_{ij}c_{jk}(\theta^{jk}_{n,s})_j], \tag{A14}$$

$$2\kappa_{xyj} = \frac{1}{d_j}[(c_{ij}c_{jk} - s_{ij}s_{jk})(\theta^{ij}_{s,s})_j + (s_{ij}c_{jk} + c_{ij}s_{jk})(\theta^{ij}_{n,s})_j$$
$$-(c_{ij}c_{jk} - s_{ij}s_{jk})(\theta^{jk}_{s,s})_j - (c_{ij}s_{jk} + s_{ij}c_{jk})(\theta^{jk}_{n,s})_j].$$

Our final task is to substitute the expressions (A6) or (A7) of the derivatives of the tangential rotations and the expressions (A8) of the derivatives of the normal rotations into equations (A14). As the result of this operation, the nodal curvatures have been expressed in terms of the nodal deflections and rotations and the shear parameters.

The result is expressed in matrix form in equation (8), where the column vectors of the nodal curvatures and the column vector of the nodal deflections and rotations are given in equations (9) and the column vector of the shear parameters in equations (10). The elements of matrix **A** can be obtained using equations

$$A_{3j-2,3i-2} = -\frac{6c_{ij}s_{jk}}{d_j h_{ij}^2},$$

$$A_{3j-2,3i-1} = -\frac{s_{jk}}{d_j h_{ij}}(2c_{ij}^2 - s_{ij}^2),$$

$$A_{3j-2,3i} = -\frac{3s_{ij}s_{jk}c_{ij}}{d_j h_{ij}},$$

$$A_{3j-2,3j-2} = +\frac{6}{d_j}(\frac{c_{ij}s_{jk}}{h_{ij}^2} - \frac{s_{ij}c_{jk}}{h_{ij}^2}),$$

$$A_{3j-2,3j-1} = -\frac{1}{d_j}[\frac{s_{jk}}{h_{ij}}(4c_{ij}^2 + s_{ij}^2) + \frac{s_{ij}}{h_{jk}}(4c_{jk}^2 + s_{jk}^2)],$$

$$A_{3j-2,3j} = -\frac{3s_{ij}s_{jk}}{d_j}(\frac{c_{ij}}{h_{ij}} + \frac{c_{jk}}{h_{jk}}),$$

$$A_{3j-2,3k-2} = +\frac{6s_{ij}c_{jk}}{d_j h_{jk}^2},$$

$$A_{3j-2,3k-1} = -\frac{s_{ij}}{d_j h_{jk}}(2c_{jk}^2 - s_{jk}^2),$$

$$A_{3j-2,3k} = -\frac{3s_{ij}s_{jk}c_{jk}}{d_j h_{jk}},$$

$$A_{3j-1,3i-2} = +\frac{6s_{ij}c_{jk}}{d_j h_{ij}^2},$$

$$A_{3j-1,3i-1} = +\frac{3s_{ij}c_{jk}c_{ij}}{d_j h_{ij}},$$

$$A_{3j-1,3i} = +\frac{c_{jk}}{d_j h_{ij}}(2s_{ij}^2 - c_{ij}^2),$$

$$A_{3j-1,3j-2} = -\frac{6}{d_j}(\frac{s_{ij}c_{jk}}{h_{ij}^2} - \frac{c_{ij}s_{jk}}{h_{jk}^2}),$$

$$A_{3j-1,3j-1} = +\frac{3c_{jk}c_{ij}}{d_j}(\frac{s_{ij}}{h_{ij}} + \frac{s_{jk}}{h_{ik}}),$$

$$A_{3j-1,3j} = +\frac{1}{d_j}[\frac{c_{jk}}{h_{ij}}(4s_{ij}^2 + c_{ij}^2) + \frac{c_{ij}}{h_{jk}}(4s_{jk}^2 + c_{jk}^2)],$$

$$A_{3j-1,3k-2} = -\frac{6c_{ij}s_{jk}}{d_j h_{jk}^2},$$

$$A_{3j-1,3k-1} = +\frac{3c_{ij}s_{jk}c_{jk}}{d_j h_{jk}},$$

$$A_{3j-1,3k} = +\frac{c_{ij}}{d_j h_{jk}}(2s_{jk}^2 - c_{jk}^2),$$

$$A_{3j,3i-2} = +\frac{6}{d_j h_{ij}^2}(c_{ij}c_{jk} - s_{ij}s_{jk}),$$

$$A_{3j,3i-1} = +\frac{1}{d_j h_{ij}}[c_{jk}(2c_{ij}^2 - s_{ij}^2) - 3s_{ij}s_{jk}c_{ij}],$$

$$A_{3j,3i} = -\frac{1}{d_j h_{ij}}[s_{jk}(2s_{ij}^2 - c_{ij}^2) - 3c_{ij}c_{jk}s_{ij}],$$

(A15)

$$A_{3j,3j-2} = +\frac{6(s_{12}s_{jk} - c_{12}c_{jk})}{d_j}(\frac{1}{h_{12}^2} - \frac{1}{h_{jk}^2}),$$

$$A_{3j,3j-1} = +\frac{1}{d_j}[\frac{c_{jk}}{h_{ij}}(4c_{ij}^2 + s_{ij}^2) + \frac{c_{ij}}{h_{jk}}(4c_{jk}^2 + s_{jk}^2) - 3s_{ij}s_{jk}(\frac{c_{ij}}{h_{ij}} + \frac{c_{jk}}{h_{jk}})],$$

$$A_{3j,3j} = -\frac{1}{d_j}[\frac{s_{jk}}{h_{ij}}(4s_{ij}^2 + c_{ij}^2) + \frac{s_{ij}}{h_{jk}}(4s_{jk}^2 + c_{jk}^2) - 3c_{ij}c_{jk}(\frac{s_{ij}}{h_{ij}} + \frac{s_{jk}}{h_{jk}})],$$

$$A_{3j,3k-2} = -\frac{6}{d_j h_{jk}^2}(c_{ij}c_{jk} - s_{ij}s_{jk}),$$

$$A_{3j,3k-1} = +\frac{1}{d_j h_{jk}}[c_{ij}(2c_{jk}^2 - s_{jk}^2) - 3s_{ij}s_{jk}c_{jk}],$$

$$A_{3j,3k} = -\frac{1}{d_j h_{jk}}[s_{ij}(2s_{jk}^2 - c_{jk}^2) - 3c_{ij}c_{jk}s_{jk}]$$

and cyclic permutation. The nonzero elements of matrix $\mathbf{B}^e$ are obtained using equations

$$B_{3j-2,i} = -\frac{6c_{ij}s_{jk}}{d_j h_{ij}},\ B_{3j-2,j} = -\frac{6s_{ij}c_{jk}}{d_j h_{jk}},$$

$$B_{3j-1,i} = +\frac{6s_{ij}c_{jk}}{d_j h_{ij}},\ B_{3j-1,j} = +\frac{6c_{ij}s_{jk}}{d_j h_{jk}}, \tag{A16}$$

$$B_{3j,i} = -\frac{6(s_{ij}s_{jk} - c_{ij}c_{jk})}{d_j h_{ij}},\ B_{3i,j} = -\frac{6(s_{ij}s_{jk} - c_{ij}c_{jk})}{d_j h_{jk}}$$

for the $n-$parameter shear approximation and using equations

$$B_{3j-2,1} = -\frac{6}{d_j}(\frac{c_{ij}^2 s_{jk}}{h_{ij}} + \frac{s_{ij}c_{jk}^2}{h_{jk}}),\ B_{3j-2,1} = -\frac{6s_{ij}s_{jk}}{d_j}(\frac{c_{ij}}{h_{ij}}\gamma_y^e + \frac{c_{jk}}{h_{jk}}),$$

$$B_{3j-1,1} = +\frac{6c_{ij}c_{jk}}{d_j}(\frac{s_{ij}}{h_{ij}} + \frac{s_{jk}}{h_{jk}}),\quad B_{3j-1,1} = +\frac{6}{d_j}(\frac{s_{ij}^2 c_{jk}}{h_{ij}} + \frac{c_{ij}s_{jk}^2}{h_{jk}}), \tag{A17}$$

$$B_{3j,1} = -\frac{6(s_{ij}s_{jk} - c_{ij}c_{jk})}{d_j}(\frac{c_{ij}}{h_{ij}} + \frac{c_{jk}}{h_{jk}}),\ B_{3i,2} = -\frac{6(s_{ij}s_{jk} - c_{ij}c_{jk})}{d_j}(\frac{s_{ij}}{h_{ij}} + \frac{s_{jk}}{h_{jk}})$$

for the $2-$parameter shear approximation, respectively, and cyclic permutation.

**Appendix B:** The nodal shears in terms of the shear parameters

We consider both the $n-$parameter shear approximation and the $2-$parameter shear approximation. Based on equations (A.1) the tangential shears of sides $ij$ and $jk$ in terms of the nodal shears of node $j$ are

$$\begin{aligned} \gamma_s^{ij} &= c_{ij}\gamma_{xj} + s_{ij}\gamma_{yj}, \\ \gamma_s^{jk} &= c_{jk}\gamma_{xj} + s_{jk}\gamma_{yj}. \end{aligned} \tag{B1}$$

Inversely the nodal shears of node $j$ in terms of the tangential shears of element sides $ij$ and $jk$ are

$$\begin{aligned} \gamma_{xj} &= \frac{1}{d_j}(s_{jk}\gamma_s^{ij} - s_{ij}\gamma_s^{jk}), \\ \gamma_{yj} &= \frac{1}{d_j}(-c_{jk}\gamma_s^{ij} + c_{ij}\gamma_s^{jk}). \end{aligned} \tag{B2}$$

Using equations (B2) and cyclic permutation, the result of the $n-$parameter shear approximation is obtained. For the $2-$parameter shear approximation case we get directly

$$\left.\begin{aligned} \gamma_{xj} &= \gamma_x^e \\ \gamma_{yj} &= \gamma_y^e \end{aligned}\right\} \; i = 1, \cdots, n. \tag{B3}$$

The obtained results can be written in matrix form (11). The nonzero element of matrix $\mathbf{C}^e$ in the $n-$parameter shear approximation are obtained using equations

$$C_{2j-1,i} = \frac{s_{jk}}{d_j},\; C_{2j-1,j} = -\frac{s_{ij}}{d_j},\; C_{2j,i} = -\frac{c_{jk}}{d_j},\; C_{2j,j} = \frac{c_{ij}}{d_j} \tag{B4}$$

and cyclic permutation. Matrix $\mathbf{C}^e$ in the $2-$parameter shear approximation is simply

$$\underset{2n\times 1}{\mathbf{C}^e} = \begin{bmatrix} 1 & 0 & \cdots & 1 & 0 \\ 0 & 1 & \cdots & 0 & 1 \end{bmatrix}^T. \tag{B5}$$